Theoretical investigation of germane and germylene decomposition kinetics

Daniela Polino, Alessandro Barbato and Carlo Cavallotti*

Received 2nd February 2010, Accepted 10th June 2010
DOI: 10.1039/c002221g

The dissociation kinetics of germane and its decomposition products were studied determining microcanonical kinetic constants with RRKM theory and integrating the master equation using a stochastic approach. Relevant reaction parameters were calculated through first principles calculations. Structures of reactants and transition states were determined at the B3LYP/aug-cc-pvtz level while energies were computed at the CCSD(T) level and extended to the complete basis set limit. Though similar for many aspects to the kinetics of decomposition of SiH_4, GeH_4 has some peculiar features that indicate a different chemical reactivity. It was found that the main decomposition channel leads to the formation of germylene, GeH_2, which rapidly decomposes to atomic Ge and H_2. The dissociation of GeH_2 to Ge and H_2 is a formally spin forbidden reaction characterized by an activation energy of 160.3 kJ mol^{-1} calculated at the minimum energy crossing point between the singlet and triplet states. The intersystem crossing probability was explicitly included in the microcanonical simulations through Landau–Zener theory. It was found that its effect on the reaction rate is almost negligible, both because of the large spin–orbit coupling between the singlet and triplet states and for the fall off conditions prevailing in the examined pressure and temperature ranges. Kinetic constants of the main decomposition channels were determined as a function of pressure and temperature between 0.0013 and 10 bar and 1100 and 1700 K. The high and low pressure kinetic constants for GeH_4 decomposition are 6.4×10^{13} $(T/\mathrm{K})^{0.272}$ $\exp(-26\,700\ \mathrm{K}/T)$ and 2.7×10^{48} $(T/\mathrm{K})^{-9.05}$ $\exp(-31\,600\ \mathrm{K}/T)$, while those for GeH_2 are 6.02×10^{12} $(T/\mathrm{K})^{0.203}$ $\exp(-19\,660\ \mathrm{K}/T)$ and 1.6×10^{26} $(T/\mathrm{K})^{-3.06}$ $\exp(-21\,121\ \mathrm{K}/T)$, respectively. A quantitative agreement with experimental data for GeH_4 decomposition could be obtained adopting a downward energy transfer parameter of $340 \times (T/298\ \mathrm{K})^{0.85}$ cm^{-1} in the collisional model, and assuming that atomic Ge can react fast with GeH_4 to form Ge_2H_2 and H_2, thus enhancing the germane decomposition rate and suggesting that a fast kinetic route leading to the Ge_2H_2 production can be active in the gas phase.

Introduction

Germane is among the most adopted gases for the chemical vapour deposition (CVD) of germanium or silicon/germanium thin films used in the manufacturing of semiconductor devices, such as diodes or transistors. The optimization of the Si/Ge growth processes can be facilitated by an accurate knowledge of germane thermochemistry and kinetics.[1] This has motivated considerable research in this field, so that several studies on the molecular properties of germane and its decomposition products can be found in the literature.[2–22] Thermochemistry was among the first germane properties to be investigated. The heat of formation of GeH_4 was experimentally determined for the first time through bomb calorimetric measurement in 1961 by Gunn and Green[9] (90.4 ± 2 kJ mol^{-1} at 298 K). Successively, Ruscic *et al.*[16] estimated heats of formation and Ge–H bond energies of GeH_4, GeH_3, GeH_2, and GeH through photoionization mass spectrometry. The GeH_3–H bond energy determined at 0 K was 343.3 ± 8.4 kJ mol^{-1}, thus in good agreement with the value determined by Reed and Brauman[23] (339.1 ± 15.5 kJ mol^{-1} at 0 K), who derived the bond energy by measuring the GeH_4 gas-phase acidity. Also Noble and Walsh,[14] investigating the iodination of germane, determined a similar value for the bond dissociation energy of the first hydrogen atom of GeH_4 (345.4 ± 8.4 kJ mol^{-1} at 0 K). According to Berkowitz *et al.*,[24] who reviewed the field, the bond energy determined by photoionization mass spectrometry is the most accurate. Almost no experimental data are available for the other GeH_x hydrides, made exception for the bond energy of 276.3 kJ mol^{-1} determined by Ruscic *et al.*[16] for the GeH–H bond.

The GeH_x thermochemical data determined through experiments were confirmed by early theoretical studies performed using several high level *ab initio* theories, going from MP2 to the hybrid G1 and G2 computational schemes.[2,13,25] Recently, Duchowicz and Cobos[6] determined the enthalpies of formation of germane and of its fluoro–chloro derivatives at the G3//B3LYP level. In the same work bond dissociation energies and barrier heights were estimated for the lowest dissociations

Dept. di Chimica, Materiali e Ingegneria Chimica "G. Natta", Politecnico di Milano, Via Mancinelli 7, 20131 Milano, Italy. E-mail: carlo.cavallotti@polimi.it; Fax: +39-02-23993180; Tel: +39-02-23993176

pathways at 0 K. Wang and Zhang[20] investigated the homolytic dissociation of germane and of its fluoro–chloro derivatives at the same level of theory. Ricca and Bauschlicher[15] computed the heats of formation for the GeH_n and Ge_2H_n species using coupled cluster theory including single double and a perturbative estimation of triple excitations (CCSD(T)) with extrapolation to the complete basis set limit (CBS) introducing corrections for spin orbital, thermal and scalar relativistic effects. Also Koizumi *et al.*[11] evaluated the heat of formation of germane at the CCSD(T) level of theory at the complete basis set limit, with explicit calculation of relativistic effects, core valence correlation, spin orbital effect and zero-point energy. Finally, Chambreau and Zhang[3] determined the energies of the thermal decomposition reactions of germane at the G3 level of theory with geometries and zero-point energies determined at the QCISD/cc-pVTZ level. These studies showed that energy and structures of GeH_x molecules can be calculated at a quantitative level of accuracy if molecular structures are determined at least at the density functional theory (DFT) level and if energies are computed adopting a high level theory, such as couple cluster or configuration interaction, and large basis sets. The calculated GeH_x–H bond dissociation energies are compared to those determined in the present work in the Results and discussion section.

While germane thermodynamics is well established, only a few experimental and theoretical works are available in the literature on its decomposition kinetics.[25–28] These studies revealed that the germane decomposition mechanism is similar to that of silane for many aspects. Its main reaction step is the dissociation to GeH_2 and H_2, which mimics the SiH_4 dissociation reaction to SiH_2 and H_2. Furthermore, both reactions proceed through a well defined tight transition state. In the present investigation we also considered as competitor channel the simple dissociation of GeH_4 to GeH_3 and H, in analogy with our recent study on SiH_4 decomposition kinetics.[29] Thus, the decomposition of GeH_4 can be described as a combination of two processes:

$$(R1)\ GeH_4 \rightarrow GeH_3 + H \qquad (1)$$

$$(R2)\ GeH_4 \rightarrow GeH_2 + H_2 \qquad (2)$$

Reaction (2) was first proposed as the germane main decomposition channel by Newman *et al.*[26] This conclusion was based on an experimental investigation of GeH_4 thermal decomposition through a single pulse shock tube operating at 5.3 bar in the 950–1060 K temperature range. Successively Newman *et al.* analyzed the overall reaction stoichiometry and found it to be:

$$GeH_4 \rightarrow Ge + 2H_2$$

Thus, it was reasonably hypothesized that reaction (2) is followed by GeH_2 decomposition through one of (or both) the following reactions:

$$(R3)\ GeH_2 \rightarrow GeH + H \qquad (3)$$

$$(R4)\ GeH_2 \rightarrow Ge + H_2 \qquad (4)$$

The analysis of the experimental results lead to the conclusion that the decomposition of GeH_2 is about 9 times faster than that of GeH_4. Votintsev *et al.*[30] studied the kinetics of germane decomposition, conducing shock tube experiments and detecting the formation of Ge atoms through atomic absorption spectrometry at 1.5 bar in the 1060–1300 K temperature range. The possibility to measure the formation of atomic germanium allowed the authors to further assess the reaction mechanism. It was thus confirmed that reactions (2) and (4) are the most important steps and that reaction (2) is the rate determining step of the overall decomposition process. More recently Smirnov[27] expanded the results of his previous study carrying out experiments at similar pressures and temperatures measuring chemiluminescence kinetics during germane dissociation behind shock waves. This work confirmed the results obtained by Votintsev *et al.*[30] A rate expression for reaction (4) was also proposed for the first time.

From a theoretical standpoint, only one work carried out by Simka *et al.*[25] investigated directly the decomposition kinetics of germane. Calculations were performed at the MP2 level to determine molecular structures and thermochemical data, while kinetic constants were calculated with classic transition state theory. Pressure effects were determined using RRKM theory as implemented in the Unimol suite of programs.[31]

Neither experimental nor theoretical kinetic data could be found for reactions (1) and (3), which are thus investigated for the first time in the present study.

In this framework we decided to study germane thermal decomposition in order to improve our understanding of this important process. In particular we calculated the kinetic constants for the decomposition of GeH_4 through reactions (1) and (2) and for GeH_2 decomposition through reactions (3) and (4) adopting a combined RRKM/master equation approach using data determined through *ab initio* calculations. The results of the calculations were then validated through comparison with literature experimental data. The paper is organized in two sections. In the Method section are reported the details about *ab initio* theories used to perform the calculations and the kinetic theory level adopted to compute the rate constants. Then, in the Results and discussion section, we report first the results of *ab initio* and high pressure kinetic constants calculations and successively the results of the master equation investigation of the GeH_4 and GeH_2 decomposition kinetics.

Method and theoretical background

The chemical reactivity of GeH_4 and GeH_2 was investigated adopting potential energy surfaces (PES) determined through *ab initio* calculations. Structures of reactants, transition states and reaction products were calculated both using density functional theory (DFT) with B3LYP functionals[32,33] and the augmented correlation consistent aug-cc-pVTZ basis set[34] and at the CASPT2 level with the cc-pVTZ basis set. Vibrational frequencies of relevant wells and transition states were determined at the B3LYP/auc-cc-pVTZ level of theory without adopting correction factors. Energies were calculated at the CCSD(T)[35] level using the aug-cc-pVTZ and aug-cc-pVQZ basis sets for wells and transition states

and then extrapolated to the infinite basis set adopting the scheme suggested by Martin as:[36]

$$E(\infty) = E(l_{\max}) - B/(l_{\max} + 1)^4 \quad (5)$$

in which $l_{\max}$ is the basis set maximum angular momentum quantum number (4 and 3 for the aug-cc-pVQZ and aug-cc-pVTZ basis sets, respectively) and B a proportionality constant that can be calculated solving eqn (5) for the two $l_{\max}$ values on which the infinite basis set extension is performed. All energies were corrected with zero point energies (ZPE) calculated at the B3LYP/aug-cc-pvtz level. The overall expression adopted to calculate the energy was thus:

$$\begin{aligned} E(\infty) = {} & E(\text{CCSD(T)/aug-cc-pVQZ}) + 0.6938 \\ & \times [E(\text{CCSD(T)/aug-cc-pVQZ}) \\ & - E(\text{CCSD(T)/aug-cc-pVTZ})] \\ & + \text{ZPE(B3LYP/aug-cc-pvtz)} \end{aligned} \quad (6)$$

The analysis of the PES of the reactions of decomposition of GeH_4 and GeH_2 to GeH_3 and GeH showed that they do not have a chemical barrier, and thus a transition state. The kinetic constants of these reactions were thus determined using the microvariational form of transition state theory on a PES determined adopting an *ab initio* theory with multireference character, which can account more properly for the contribution of virtual orbitals to the molecular wave function than a single reference approach, such as DFT or CCSD(T). Thus intermediate structures and energies were calculated as a function of the reaction coordinate at the CASPT2[37,38] level using the cc-pVQZ basis set including in the active space all the valence electrons. Frequencies were computed at the same level of theory. CASPT2 energies were then re-scaled to fit the overall binding energy determined at the CCSD(T) level, which was found in this and previous studies to predict bond energies that are in good agreement with those experimentally measured.[15] All DFT calculations were carried out adopting the Gaussian 03 computational suite,[39] while CASPT2 and CCSD(T) calculations were performed adopting the Molpro 2008.1 computational suite.[40]

RRKM microcanonical rate constants $k(E,J)$ were computed from the convoluted rotational and vibrational density of states as a function of energy E and angular momentum J. All the vibrational and external rotational degrees of freedom were considered in the calculation of $k(E,J)$ for reactions with a chemical barrier. This is based on the hypothesis that the intramolecular rotational–vibrational energy transfer is fast. The high pressure rate coefficients were calculated both integrating $k(E,J)$ over the Boltzmann population and from the classic TST expression, as they give the same result. The approach adopted to determine $k(E,J)$ for the reactions proceeding without passing from a chemical barrier is the E,J model proposed by Miller *et al.*[41] This approach, formally similar to that used for reactions proceeding through a chemical barrier as it treats all rotational degrees of freedom as active, was compared to an alternative approach in which the external degrees of freedom are distinguished between active and nonactive by Miller *et al.*[41] The E,J model proved to be superior in predicting energy transfer parameters and was therefore implemented in our code. Also, it has the advantage of directly predicting the high pressure limit without need of introducing any correction factor for the inactive external rotational degrees of freedom.

The density of states related to the transitional GeH_3–H and GeH–H bending motions were treated in the harmonic oscillator approximation using the vibrational frequencies calculated at the CASPT2 level. A similar approach applied to the study of the decomposition of CH_4 to CH_3 and H led to a good fit of experimental data. Despite this, the harmonic approximation is probably unreal for this class of reactions and we plan in the near future to update our computational approach by implementing a hindered rotor approximation. However, as will be discussed later on, the present calculations predict that decomposition to GeH_3 and GeH has a minor impact on the overall decomposition kinetics and therefore the uncertainty associated to the above assumption is likely to have a small influence on the overall rate constants calculated in the present work.

The transition state for reaction (4) takes place in correspondence of the Minimum Energy Crossing Point (MECP) of the singlet and triplet PES of GeH_2 and is therefore formally spin forbidden.[42] The singlet–triplet transition of GeH_2 has been the subject of several theoretical studies in the literature and it is expected to proceed fast because of the large spin–orbit coupling between the two states.[43] The probability of intersystem crossing was included in our microcanonical calculation by evaluating the $k(E,J)$ microcanonical rate as:

$$k(E,J) = \frac{\int_0^{E-E_0} \rho^{\neq}(E^I,J) p_{\text{hop}}(E - E_0 - E^I) \mathrm{d}E^I}{h\rho(E,J)} \quad (7)$$

where ρ is the density of states, J the angular momentum, E the rovibrational energy, and p_{hop} the probability of intersystem hopping, which was calculated from Landau–Zener theory[44] as the probability of hopping in a double pass through the MECP as:[42]

$$p_{\text{hop}}(E) = (1 - P_{\text{LZ}})(1 + P_{\text{LZ}}) \quad (8)$$

in which the Landau–Zener transition probability was calculate as:[44]

$$P_{\text{LZ}} = \exp\left(-\frac{2\pi H_{\text{SO}}^2}{\hbar \Delta F}\sqrt{\frac{\mu}{2E}}\right) \quad (9)$$

where H_{SO} is the off-diagonal spin–orbit coupling element of the 4 × 4 Hamiltonian matrix between the singlet and triplet state, ΔF is the relative slope of the triplet and singlet PES at the MECP, μ is the reduced mass of the reacting moieties, and E is the system kinetic energy. The spin–orbit matrix element H_{SO} was calculated adopting spin–orbit singlet and triplet wave functions determined using multireference configuration interaction (MRCI) theory including all valence electrons in the active space adopting the cc-pVTZ basis set.[40,45] The forces at the MECP were calculated at the B3LYP/aug-cc-pvtz level.

Master equation (ME) calculations were performed adopting the 1D master equation formulation proposed by Miller *et al.*,[41] which was derived by J-averaging the E,J 2D

master equation and is implemented in our computational code as described in detail in Barbato *et al.*[29] Briefly, the code is based on the stochastic integration of the master equation, which is performed discretizing the investigated rovibrational energy field into finite bins whose reacting properties were determined with RRKM theory.

Results and discussion

The results are presented in two sections. In the first we report and discuss the *ab initio* simulations and the calculation of high pressure rate constants adopting classic transition state theory and microvariational *J*-resolved transition state theory, while in the second we report the results of the investigation of the pressure dependence of the decomposition rate constant for the two systems considered.

Ab initio calculations and evaluation of high pressure rate constants

Energies, vibrational frequencies, structural and reaction parameters of reactants and transitions states for GeH_4, GeH_2, and reactions (2) and (4) are summarized in Table 1. The energy change and activation energies of reaction (2) were experimentally and theoretically determined by several authors and was thus used to discuss the level of accuracy of the present calculations.

Experimentally it was found that the reaction enthalpy should be higher than 147 kJ mol^{-1} [16] and it was proposed a most probable value of 163.3 kJ mol^{-1}, though the uncertainty was great (41.9 kJ mol^{-1}). Enthalpy changes determined through first principle calculations are comprised between 150.7 and 171.7 kcal mol^{-1}. The most accurate theoretical value is most likely the 157.4 kJ mol^{-1} enthalpy change determined by Ricca and Bauschlicher,[15] which includes relativistic and spin–orbit corrections as well as extension to the infinite basis set. The enthalpy change calculated in the present study, 164.5 kJ mol^{-1}, is thus in reasonable agreement with both the theoretical best estimate and the available experimental data. Also the calculated activation energy of reaction (2) (217.7 kJ mol^{-1}) is in good agreement with that experimentally evaluated by Votintsev *et al.*[28] (218.1 ± 13 kJ mol^{-1}) and Newman *et al.*[26] (209.3–227.3 kJ mol^{-1}), while it is slightly larger than that determined by Smirnov[27] (208.1 kJ mol^{-1}) and in good agreement with that computed by Simka *et al.*[25] through MP2 calculations (224.8 kJ mol^{-1}). The inverse process, the direct insertion of H_2 in GeH_2, was studied by Becerra *et al.*[46,47] The energy barrier calculated at the QCISD/6-311+G(3df,2pd) level is 57.8 kJ mol^{-1}, thus in good agreement with the 53.2 kJ mol^{-1} determined in the present study.

Few experimental studies are available in the literature on the GeH_2 decomposition thermochemistry. Ruscic *et al.*[16] determined experimentally the GeH_2 heat of formation, through which a decomposition reaction energy of 110.5 kJ mol^{-1} was determined using the heat of formation of atomic germanium experimentally evaluated by Glushko *et al.*[48] Several theoretical

Table 1 Energetic, structural and reaction parameters adopted to determine the high-pressure rate constant of reactions (2) and (4). H1 and H2 are the reacting hydrogen atoms. Wells and transition state energies are reported in Hartrees, vibrational frequencies in cm^{-1}, and rotational constants in GHz. Activation energies, reported in kJ mol^{-1}, are corrected with ZPE. Geometry parameters are evaluated at the B3LYP/aug-cc-pVTZ level. In parenthesis are displayed energies, vibrational frequencies (cm^{-1}), and geometry parameters evaluated at the CASPT2/cc-pVTZ level, which in the case of TS2 refer to the $^1B_1$ excited state

	GeH_4	TS1	GeH_2	TS2
E(B3LYP/aug-cc-pVTZ)	−2079.448136	−2079.399178	−2078.221807	−2078.166323
E(CCSD(T)/cc-pVTZ)	−2077.891355 (−2077.891437)	−2077.804709 (−2077.804727)	−2076.649686 (−2076.649245)	−2076.585637 (−2076.586958)
E(CCSD(T)/cc-pVQZ)	−2077.901066 (−2077.901132)	−2077.814192 (−2077.814154)	−2076.656941 (−2076.656556)	−2076.592733 (−2076.593934)
ZPE(B3LYP/aug-cc-pVTZ)	0.029318	0.025137	0.010716	0.00738
E(CCSD(T)/CBS + ZPE)	−2077.878486 (−2077.878540)	−2077.795635 (−2077.795558)	−2076.651259 (−2076.650912)	−2076.590276 (−2076.591395)
E_{act}(B3LYP/aug-cc-pVTZ)	—	117.6	—	136.9
E_{act}(CCSD(T)/CBS + ZPE)	—	217.8 (218.0)	—	160.3 (156.4)
Distance Ge–H1/Å	1.53 (1.54)	1.57 (1.58)	1.60 (1.57)	1.75 (1.79)
Distance Ge–H2/Å	1.53 (1.54)	1.72 (1.75)	1.60 (1.57)	1.75 (1.79)
Distance H1–H2/Å	2.51 (2.52)	1.25 (1.22)	2.28 (2.26)	0.99 (1.10)
Angle H1–Ge–H2	109.5 (109.5)	44.3 (42.6)	90.9 (92.0)	32.9 (35.8)
Vibrational frequencies				
1	824.8 (826.9)	i1248.8 (i1231.1)	935.3 (932.0)	i1449.7 (i1148.4)
2	824.8 (826.9)	649.4 (647.6)	1880.6 (1910.3)	1486.9 (1214.3)
3	824.8 (826.9)	713.4 (691.0)	1888.0 (1913.3)	1752.3 (1514.7)
4	925.8 (918.4)	881.6 (874.6)	—	—
5	925.8 (918.4)	943.1 (939.4)	—	—
6	2130.2 (2141.6)	1556.0 (1448.9)	—	—
7	2137.6 (2141.6)	2056.7 (2042.5)	—	—
8	2137.6 (2141.6)	2105.0 (2095.8)	—	—
9	2137.6 (2143.8)	2128.8 (2115.9)	—	—
Rotational constant (GHz) I1	79.9	92.9	205.0	1021.0
Rotational constant (GHz) I2	79.9	73.5	193.6	91.6
Rotational constant (GHz) I3	79.9	64.0	99.6	84.1
Rotational symmetry number	12	1	2	2
Symmetry group	T_D	C_1	C_{2v}	C_{2v}

studies were dedicated to the thermochemical investigation of this reaction.[3,6,12,15,20] In particular Ricca and Bauschlicher[15] calculated an energy change of 123.9 kJ mol^{-1}, while Chambreau and Zhang[3] and Wang and Zhang[20] both determined a 117.2 kJ mol^{-1} energy change. More recently, Duchowicz and Cobos[6] computed the heats of formation of germane derivatives with the alternative approach of the isodesmic reaction scheme, through which they determined a reaction energy of 131.0 kJ mol^{-1}. The enthalpy change here calculated (133.5 kJ mol^{-1}) is in good agreement with that found by Duchowicz and Cobos,[6] but overestimates by about 10 kJ mol^{-1} the one determined by Ricca and Bauschlicher. The GeH_2 bond dissociation energy was determined experimentally through photoionization mass spectrometry by Ruscic *et al.*,[16] who reported an upper bound of 288.5 kJ mol^{-1} and a most probable value of 276.3 kJ mol^{-1}. This energy is slightly smaller than that calculated through first principle calculations reported in the literature,[3,5,6,20] which all fall all in a range comprised between 282.6 to 289.7 kJ mol^{-1}. The bond dissociation energy computed in the present work (291.8 kJ mol^{-1}) is thus in good agreement with the theoretical estimates and near the upper bound of the energy determined experimentally.

On the basis of the discussion reported above, we conclude that a reasonable uncertainty level of the energies computed on the GeH_4 and GeH_2 PES is about 7 and 10 kJ mol^{-1}, respectively.

The transition state for the reaction of decomposition of GeH_4 to GeH_2 and H_2 was determined both at the B3LYP/aug-cc-pvtz and CASTP2/cc-pvtz levels. It was interesting to find that the geometries determined at the two levels of theory are extremely similar, as they differ by less than 0.03 Å and that the computed activation energies are in practice undistinguishable. As there are many similarities between germane and silane, it is interesting to compare the parameters determined for the GeH_4 decomposition reaction with those calculated for SiH_4 in our previous study.[29] The transition state structures of the two reactions are shown in Fig. 1. As it can be observed, at a first sight they appear to be qualitatively similar: both structures have no rotational symmetry; the two Si–H and Ge–H bonds involved in the reactions differ only by about 0.12–0.15 Å; the two SiH and GeH bonds not participating in the reaction are positioned in a plane perpendicular to that formed by the other two bonds; the H–H distance in the GeH_4 transition state is only 0.1 Å larger than that calculated for SiH_4. Despite the similarities, the two systems differ substantially from an energetic standpoint. First, the reaction activation energy calculated at the CCSD(T) level and extrapolated to the infinite basis set is 238.6 kJ mol^{-1} for SiH_4 and 217.7 kJ mol^{-1} for GeH_4, and thus does not scale with the calculated bond dissociation energy, which is 234.5 kJ mol^{-1} for SiH_4 and 164.5 for GeH_4 (0 K bond dissociation energy corrected with zero point energy). The relatively high activation energy for the GeH_4 reaction, which is only 21 kJ mol^{-1} smaller than that determined for SiH_4 despite a reaction energy change about 71.2 kJ mol^{-1} smaller, is unlikely to be determined by the energy required to distort the reacting hydrogen atoms from their minimum energy position, as the H–H distance in SiH_4 and GeH_4, 2.421 Å and 2.505 Å, are very similar, as well as the associated bending vibrational frequencies, which are 918 and 824 cm^{-1}, respectively. A more reasonable explanation is that the formation of the hydrogen molecule is partially hindered in GeH_4 by a repulsive interaction between the electronic density of the Ge atom and that of the forming H_2 molecule, which is likely to be larger than that experienced by SiH_4, as the GeH_4 electronic density is considerably more diffuse. The presence of a significant barrier to the recombination of H_2 and GeH_2 is likely to favor the formation of this reactive species in atmospheres in which the hydrogen concentration is relatively high and will hinder the attainment of chemical equilibrium between GeH_4, GeH_2 and H_2 in a reactive gas phase, since even a small activation energy will decrease exponentially the reaction rate of the GeH_2 and H_2 recombination process.

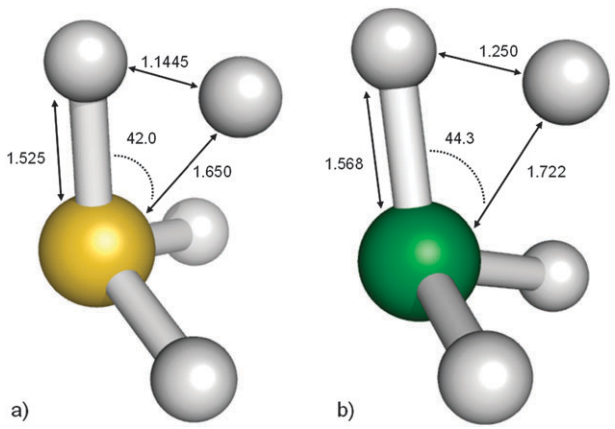

Fig. 1 Transition state structures for the reactions of decomposition of (a) SiH_4 and (b) GeH_4 to SiH_2 and GeH_2 determined at the B3LYP/aug-cc-pVTZ level. Distances in Angstrom and angles in degrees.

The transition state for the reaction of decomposition of GeH_2 to Ge and H_2 was determined on the singlet PES using an unrestricted B3LYP formalism and a broken symmetry guess wavefunction. Differently from what found for GeH_4, the transition state has C_{2v} symmetry and the spin contamination $\langle S^2 \rangle$ of the converged wavefunction is 0.56, thus indicating a significant multireference character. A saddle point search performed on the GeH_2 PES at the CASTP2/cc-pvtz showed that no transition state leading to the direct dissociation of GeH_2 to Ge and H_2 could be located both on the singlet ($^1A_1$) and triplet ($^3B_1$) PES, though a transition state with a structure similar to that found using the unrestricted DFT approach, whose structural parameters are reported in Table 1, was determined for the singlet $^1B_1$ excited state. SCF energies indicate that both transition states are located in proximity of the conical intersection of the triplet and singlet PES, which implies that the progress of the reaction requires intersystem crossing between the singlet and triplet states. The hopping probability was determined as described in the Method section using Landau–Zener theory. The spin–orbit matrix element H_{SO} calculated at the MECP is 282 cm^{-1}, thus in good agreement with the

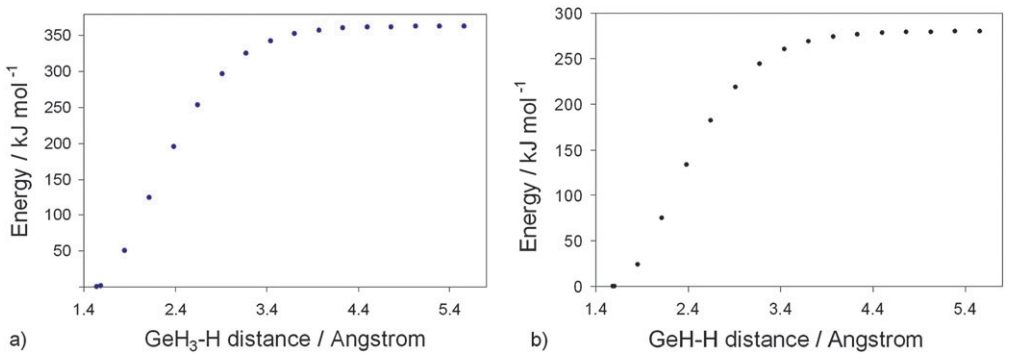

Fig. 2 PES of the GeH_4 (a) and GeH_2 (b) reactions of dissociation to GeH_3 and GeH calculated at the CASTP2 level using the cc-pVQZ basis set and corrected with ZPE calculated using vibrational frequencies determined at the same level of theory.

310 cm^{-1} determined by Matsunaga *et al.*[43] for GeH_2 using a relativistic potential energy surface and an effective core potential basis set. The difference between the forces acting on the two states, calculated at the B3LYP/aug-cc-pvtz level, is 115.6 kJ mol^{-1} $Å^{-1}$. Given the high spin coupling value, it is reasonable to expect that the hopping probability is fast and that it will not affect considerably the system reactivity. This is indirectly confirmed by the good agreement found between the calculated and experimental activation energies. The activation energy calculated for reaction (4) (160.2 kJ mol^{-1}) in fact only slightly overestimates that evaluated by Votintsev[28] ($\lesssim$146.9 kJ mol^{-1}) and Smirnov[27] (134.8 kJ mol^{-1}), both determined by fitting of experimental data.

For the dissociation of GeH_4 and GeH_2 to GeH_3 and GeH we determined the rate constants in the high pressure limit adopting microvariational transition state theory on the PES calculated at the CASPT2 level. The PES for GeH_4 and GeH_2 homolytic decomposition reactions are sketched in Fig. 2 as a function of the length of the breaking bond. According to Berkowitz *et al.*,[24] the best estimate of the GeH_3–H bond energy, determined through photoionization mass spectrometry, is 344.1 ± 8.4 kJ mol^{-1} at 0 K. This result was confirmed by several theoretical studies, which reported values comprised between 355.9 and 347.9 kJ mol^{-1},[2,3,5–8,13,15,20] and by the present calculations (349.6 kJ mol^{-1}).

The high pressure kinetic constants were calculated for reactions (1)–(4) using both classic and microcanonical transition state theory. The kinetic constants determined using the microcanonical approach were interpolated between 300 and 2200 K and are reported in Table 3. It was found that the *E*,*J* resolved microvariational determination of the kinetic constants of reactions (1) and (3) leads to a slight decrease of about 15% of the kinetic constants determined using classic variational transition state theory. A more significant effect was found for the spin forbidden reaction $GeH_2 \rightarrow Ge + H_2$, in which the high pressure kinetic constant decreases with respect to that determined using classic transition state

Table 3 High-pressure kinetic constants of the considered reactive events interpolated between 300 and 2200 K to the modified Arrhenius expression ($k = A(T/K)^n \exp(-E_a/R(T/K))$). Activation energies and reaction enthalpies are reported in kJ mol^{-1}. The bimolecular kinetic constant has dimensions of cm^3 mol^{-1} s^{-1}. The kinetic constant for the reaction of decomposition of GeH_2 was determined by integrating the microcanonical $k(E,J)$ rates over the Boltzmann population, and therefore accounts for the intersystem crossing probability

	A	n	E_a	ΔH (0 K)
$GeH_4 \rightarrow GeH_3 + H$	3.4×10^8	2.46	359.1	349.6
$GeH_4 \rightarrow GeH_2 + H_2$	6.4×10^{13}	0.272	221.9	164.5
$GeH_2 \rightarrow GeH + H$	1.6×10^{16}	−0.369	300.5	291.8
$GeH_2 \rightarrow Ge + H_2$	6.0×10^{12}	0.203	163.5	133.6

Table 2 Activation energies and 0 K enthalpy changes for the reaction of decomposition of GeH_4 to GeH_2 and H_2. Theoretical data corrected with ZPE. Energies expressed in kJ mol^{-1}

ΔH_0 (0 K)	E_a	Method	Reference
163.3 ± 41.9	209.3–227.3	Single pulse shock tube GeH_4 detection through mass spectrometry	Newman *et al.*[26]
> 147.0		Photoionization mass spectrometry	Ruscic *et al.*[16]
	218.1 ± 13	Shock tube Ge atoms detection by atomic absorption	Votintsev *et al.*[28]
	208.1	Shock tube Chemiluminescence detection	Smirnov[27]
171.7	224.8	MP2/BC(1d,1f)	Simka *et al.*[25]
150.7		G3//QCISD/cc-pVTZ	Chambreau and Zhang[3]
153.1		G3//B3LYP/6-31G(2df,p)	Wang and Zhang[20]
152.8	208.1	G3//B3LYP/6-31G(2df,p)	Duchowicz and Cobos[6]
165.8		MP4/962(d,p)//HF/641(d)	Binning and Curtiss[2]
157.4		CCSD(T)/CBS//B3LYP/6-311 + + G(2df,2p)	Ricca and Bauschlicher[15]
165	218	QCISD(T)/6-311G + + (3df,2pd)// QCISD/6-311G(d,p)	Becerra *et al.*[47]
164.5	217.7	CCSD(T)/CBS//CASPT2/aug-cc-pVTZ	This work

theory by a factor of about 2 because of the inclusion of the intersystem crossing probability in the calculations.

GeH_4 and GeH_2 decomposition kinetics

The GeH_4 and GeH_2 decomposition kinetics was studied integrating the master equation for a pure Argon bath gas, adopting an exponential down model for the collisional energy transfer, and using as Lennard-Jones collision parameters for bath gas and reactants the literature values of $\sigma = 3.75$ Å and $\varepsilon = 98.3\ cm^{-1}$ for Argon, and $\sigma = 4.30$ Å and $\varepsilon = 166.1\ cm^{-1}$ for GeH_4.[49] The Lennard-Jones parameters of GeH_2 were determined scaling those of GeH_4 as they scale for SiH_4 with respect to SiH_2. The values so determined are $\sigma = 3.93$ Å and $\varepsilon = 106.3\ cm^{-1}$. Since energy transfer parameters are not well known for GeH_x molecules, we assumed as first guess that the mean downward transfer energy is $170 \times (T/298\ K)^{0.85}\ cm^{-1}$ for both systems. This functional form was found to yield good agreement with experimental data for our previous investigation of the SiH_4 dissociation reaction[29] and by Matsumoto when studying the Si_2H_6 reactivity.[50] Since, among the others, this parameter is the most uncertain, its impact on the calculations was investigated through a sensitivity analysis.

The $k(E,J)$ kinetic constants were calculated at E and J steps of 1 cm^{-1} and 1, for E and J comprised between 1 and 50 000 cm^{-1} and 1 and 150, respectively. The microcanonical kinetic constants were then averaged over J as proposed by Miller *et al.*[41] and the $k(E)$ so determined were finally averaged in discrete reaction bins. The J averaged $k(E)$ RRKM kinetic constants for the reactions of dissociation of GeH_4 to GeH_2 and GeH_3 are reported in Fig. 3 as a function of the internal energy. In order to determine the effect of the bin size on the accuracy of the calculations two different tests were performed. The first was the check of the consistency of the high pressure rate constants calculated assuming a Boltzmann energy distribution both for the 1 cm^{-1} E spaced $k(E,J)$ kinetic constants and for those averaged over 100 cm^{-1} bins. The high pressure rate constants calculated using the microcanonical $k(E,J)$ kinetic constants and the J-averaged kinetic constants were always in quantitative agreement with those determined using classic transition state theory

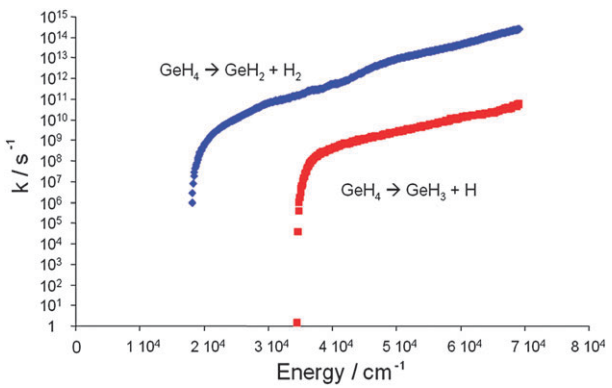

Fig. 3 Microcanonical RRKM kinetic constants calculated for the reaction of decomposition of GeH_4 to GeH_2 and GeH_3, reported in s^{-1}.

(*i.e.* when no intersystem crossing was considered), while those determined with the 100 cm^{-1} binned rate constants differed by the expected values by no more than 5%. The second test consisted in performing several simulations (*i.e.* GeH_4 and GeH_2 decomposition between 1100 and 1700 K at 1 bar) by systematically reducing the bin size to 50 and 25 cm^{-1}. It was found that the effect of the bin size is negligible (*i.e.* the deviation from the 100 cm^{-1} reference value is smaller than 5%) as long as the maximum energy change allowed for a single jump is at least 4500 cm^{-1}, which corresponds to a max jump parameter of 45 (which means that a maximum of 92 transitions are stored in the binary tree for each stochastic event).

Simulations were performed studying explicitly the dynamics of N parallel systems, each composed by a single molecule, starting the simulations from an unexcited state. The pressure dependent kinetic constant was then determined by regression over the reaction time, using the linear regression algorithm over reacted molecules as a function of reaction time we recently introduced.[29] The number of reactive events needed to reach a converged solution was determined dynamically, as it changes with temperature and pressure, by adopting as convergence parameter the student's t-test with a 1% confidence limit.[29] At least about 500 events and 10^8 random transitions were generally necessary to reach converged solutions for most simulations. Simulations were performed for temperatures comprised between 1100 and 1700 K and pressures comprised between 10^{-3} and 10 bar. Some specific simulations were performed at 1600 K and at 1700 K at increasing pressures to check both the internal consistency of the code in terms of capability to predict the high pressure limit as well as to determine the pressure at which the high pressure limit is finally reached. The calculated kinetic constants reached smoothly the limiting rates for pressures of about 2×10^4 bar for both simulation sets. The calculated high pressure rate constants were about 95% of those computed with TST, which confirms that the stochastic code is able to predict the correct high pressure behavior for the conditions in which the Boltzmann equilibrium distribution is reached.

The calculated RRKM/ME rate constants for GeH_4 and for GeH_2, reported in Tables 4 and 5, are sketched in Fig. 4 and compared to experimental data in Fig. 5. Interestingly, we did not observe any reactive event leading to the direct decomposition of GeH_4 to GeH_3 and H in the investigated temperature and pressure range. This result could in part be expected since, analyzing the high pressure rate constants of these reactions, it can be observed that the rate constant of the simple dissociation reaction is from 5 to 2 orders of magnitude lower than that of the reaction that produces GeH_2 and H_2. A similar result was found also for GeH_2 decomposition. A second less evident reason is that, in the investigated temperature and pressure range, both the reactive systems considered are deep in their fall off regime. In this situation the population of the most excited states is significantly depleted with respect to the Boltzmann population, so that it is extremely difficult for an excited state to reach the reaction energy threshold of the most activated dissociation reaction. This can be directly observed from the analysis of the calculated population of the

Table 4 Calculated kinetic constant (s^{-1}) for the decomposition of GeH_4 to GeH_2 and H_2 reported in the 10^{-3}–10 bar pressure range and in the 1100–1700 K temperature range

	Pressure/bar							
T/K	0.00132	0.0132	0.132	0.6	1.0	2.0	4.5	10.0
1100	3.66	2.54×10^{1}	1.86×10^{2}	6.92×10^{2}	9.68×10^{2}	1.63×10^{3}	2.90×10^{3}	3.97×10^{3}
1200	1.65×10^{1}	1.20×10^{2}	9.75×10^{2}	3.38×10^{3}	5.34×10^{3}	8.42×10^{3}	1.41×10^{4}	2.19×10^{4}
1300	5.77×10^{1}	4.07×10^{2}	3.50×10^{3}	1.30×10^{4}	1.94×10^{4}	3.19×10^{4}	5.60×10^{4}	8.94×10^{4}
1400	1.52×10^{2}	1.15×10^{3}	1.02×10^{4}	3.8×10^{4}	5.69×10^{4}	9.95×10^{4}	1.72×10^{5}	2.89×10^{5}
1500	3.50×10^{2}	2.71×10^{3}	2.36×10^{4}	8.9×10^{4}	1.42×10^{5}	2.39×10^{5}	4.38×10^{5}	7.53×10^{5}
1600	6.82×10^{2}	5.46×10^{3}	4.73×10^{4}	1.89×10^{5}	2.94×10^{5}	5.05×10^{5}	9.34×10^{5}	1.67×10^{6}
1700	1.17×10^{3}	9.17×10^{3}	8.52×10^{4}	3.40×10^{5}	5.25×10^{5}	9.22×10^{5}	1.79×10^{6}	3.21×10^{6}

Table 5 Calculated kinetic constant (s^{-1}) for the decomposition of GeH_2 to Ge and H_2 reported in the 10^{-3}–10 bar pressure range and in the 1100–1700 K temperature range

	Pressure/bar							
T/K	0.00132	0.0132	0.132	0.6	1.0	2.0	4.5	10.0
1100	5.31	5.31×10^{1}	5.12×10^{2}	2.39×10^{3}	3.70×10^{3}	7.22×10^{3}	1.37×10^{4}	2.84×10^{4}
1200	1.84×10^{1}	1.84×10^{2}	1.77×10^{3}	7.75×10^{3}	1.15×10^{4}	2.14×10^{4}	4.43×10^{4}	9.09×10^{4}
1300	5.06×10^{1}	5.04×10^{2}	4.92×10^{3}	2.16×10^{4}	3.41×10^{4}	6.56×10^{4}	1.35×10^{5}	2.78×10^{5}
1400	1.22×10^{2}	1.21×10^{3}	1.20×10^{4}	5.18×10^{4}	8.36×10^{4}	1.60×10^{5}	3.37×10^{5}	6.73×10^{5}
1500	2.54×10^{2}	2.53×10^{3}	2.50×10^{4}	1.09×10^{5}	1.78×10^{5}	3.39×10^{5}	7.07×10^{5}	1.41×10^{6}
1600	4.63×10^{2}	4.63×10^{3}	4.56×10^{4}	2.00×10^{5}	3.26×10^{5}	6.24×10^{5}	1.33×10^{6}	2.65×10^{6}
1700	7.83×10^{2}	7.85×10^{3}	7.72×10^{4}	3.41×10^{5}	5.61×10^{5}	1.08×10^{6}	2.20×10^{6}	4.67×10^{6}

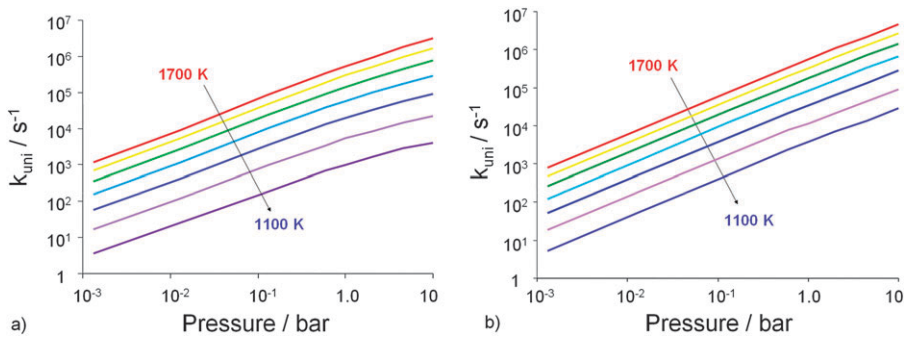

Fig. 4 Calculated kinetic constant for the decomposition of (a) GeH_4 to GeH_2 and H_2 and (b) GeH_2 to Ge and H_2.

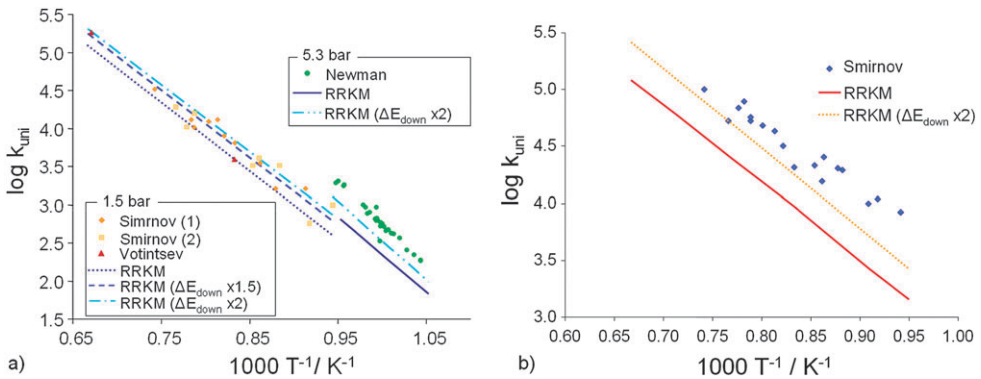

Fig. 5 (a) Comparison of the calculated kinetic constants for the decomposition of GeH_4 to GeH_2 and H_2 with the experimental data measured by Votintsev *et al.*[28] and Smirnov[27] at 1.5 bar in the presence of (1) 1.0% N_2O and (2) 3.0% N_2O and by Newman *et al.*[26] at 5.3 bar. (b) Comparison of the calculated kinetic constants for the decomposition of GeH_2 to Ge and H_2 with the experimental data measured by Smirnov[27] at 1.5 bar.

excited energy states for a GeH_4 reacting system, which is reported in Fig. 6 where it is compared with the Boltzmann population.

A specific set of simulations was performed with the aim of determining the effect that the inclusion of the intersystem crossing probability in the estimation of the microcanonical

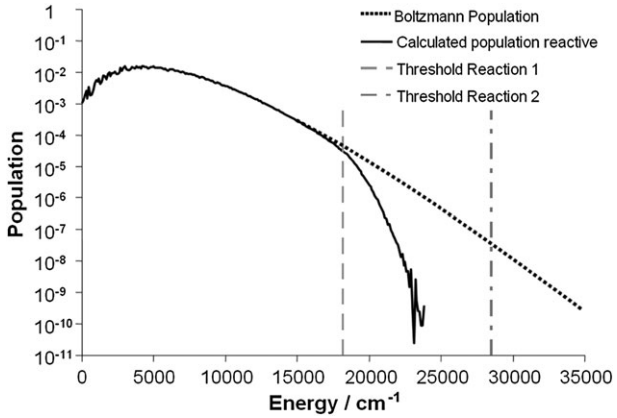

Fig. 6 Comparison between the energy distribution function calculated for the GeH_4 reactive system at 1 bar and 1400 K and the Boltzmann population. The energy thresholds for reactions (1) and (2) are shown to highlight the dramatic decrease of population of the excited states that takes place above the first reaction threshold.

kinetic constants has on the decomposition kinetics. It was interesting to find out that, though the high pressure rate constants decrease by a factor of 2 upon inclusion of the p_{hop} probability in eqn (7), the effect on the master equation simulations is much smaller, with a decrease of the kinetic constants calculated in the investigated temperature and pressure ranges of about 15% with respect to the rates computed without accounting for the intersystem crossing probability. The motivation for this small impact of intersystem crossing on the rate constant is that in the fall off regime prevailing in these conditions the high rovibrational energy levels are depleted and the reactivity is determined mostly by the energy states located just above the reaction energy threshold. For these states the kinetic energy available for the transitional modes is little, so that P_{LZ} is small and p_{hop} approaches unity.

The comparison between the RRKM/ME calculations and the first set of experimental data considered (Votintsev *et al.*[28] and Smirnov *et al.*[27]), measured over the 1060–1500 K temperature range and at a pressure of 1.5 bar, concerns the GeH_4 and GeH_2 decomposition kinetic constants and is reported in Fig. 5. As it can be observed, the calculations underpredict the measured kinetic constants by an average factor of 1.6 for GeH_4 decomposition, which more than doubles for GeH_2 decomposition. A possible explanation for the observed disagreement is the choice of the energy transfer parameter for the collision energy transfer process, on which, as mentioned above, there is considerable uncertainty. Thus we decided to perform a sensitivity analysis in order to investigate what is the effective impact of this parameter on the calculated rate constants. It was found that increasing the energy transfer up to a factor of two leads to a decrease of the difference between calculations and experimental data from a factor of 1.6 to 1.3 in the case of GeH_4 decomposition, thus within the experimental uncertainty, and from 3.5 to 1.6 for GeH_2 decomposition. Increasing the energy transfer parameter above a factor of two did not affect significantly the computational results.

Also for the second set of simulations an underestimation of experimental data, measured in a different temperature range (950–1060 K) and at a higher pressure (5.3 bar) with respect to those reported by Smirnov, was observed. The disagreement is significantly larger than that found for the first set of data simulated. The discrepancies between calculations and experiments for the data reported by Newman *et al.*[26] for the GeH_4 decomposition is in fact a factor of 2.5, which reduces to 1.7 increasing the energy transfer parameter. These differences were detected also by Simka *et al.*[25] who carried out a RRKM study of germane decomposition. The underestimation of the experimental data, a factor of 4.5, is larger than that calculated in the present study and can mostly be ascribed to the lower value of the high pressure rate constants, in which the pre-exponential is a factor of two smaller than that computed in the present work (most probably because its temperature dependence was neglected) while the activation energy is about 7 kJ mol^{-1} higher (calculations were performed at a lower level of theory, as reported in Table 2).

To further study the origin of the discrepancy between experimental and theoretical data we investigated whether it might be determined by the presence of secondary reactions. A peculiarity of this reaction system is in fact represented by the rate at which GeH_2 dissociates to Ge and H_2, which is significantly faster than the rate of dissociation of GeH_4. It becomes thus possible that, if Ge atoms react with GeH_4 sufficiently fast, they may accelerate the overall GeH_4 decomposition rate. Since it is well known that Si can react fast (with almost collisional efficiency) with SiH_4 to form Si_2H_2,[51,52] we hypothesized that a similar reaction may be active also for this system. We thus simulated both sets of experimental data adopting a kinetic scheme constituted by reactions (1)–(4) with the addition of the following reaction:

$$(R5)\ GeH_4 + Ge \rightarrow Ge_2H_2 + H_2 \qquad (10)$$

The kinetic constant adopted for reaction (5) was first assumed to be equal to that reported by Dollet and de Persis[51] for the reaction of SiH_4 with atomic Si, while for the other reactions we used the kinetic constants evaluated in this study. The simulations of the first set of experimental data did not evidence any impact of the introduction of reaction (5) on the rate of decomposition of GeH_4, also when increasing the reaction rate up to the collisional limit. The situation changed however for the second sets of experimental data, which were measured performing the experiments using an initial GeH_4 concentration significantly higher than that adopted by Smirnov. The results of the simulations are compared with experimental data in Fig. 7.

In Fig. 7a and b are reported the results of the simulations of the second set of experimental data performed adopting reactions (1)–(5) with the kinetic constants determined with the reference energy transfer parameter. As it can be observed, the presence of reaction (5) reduces the difference between the calculated and experimental data, though a certain disagreement can still be observed, especially at high temperatures. Increasing the energy transfer parameter by a factor 2, which gave a satisfactory agreement with the first experimental data set, leads also in this case to a good reproduction of the experimental data. The results are shown in Fig. 7c and d. Interestingly, a sensitivity analysis on the kinetics constant of reaction (5) revealed that even decreasing significantly its value

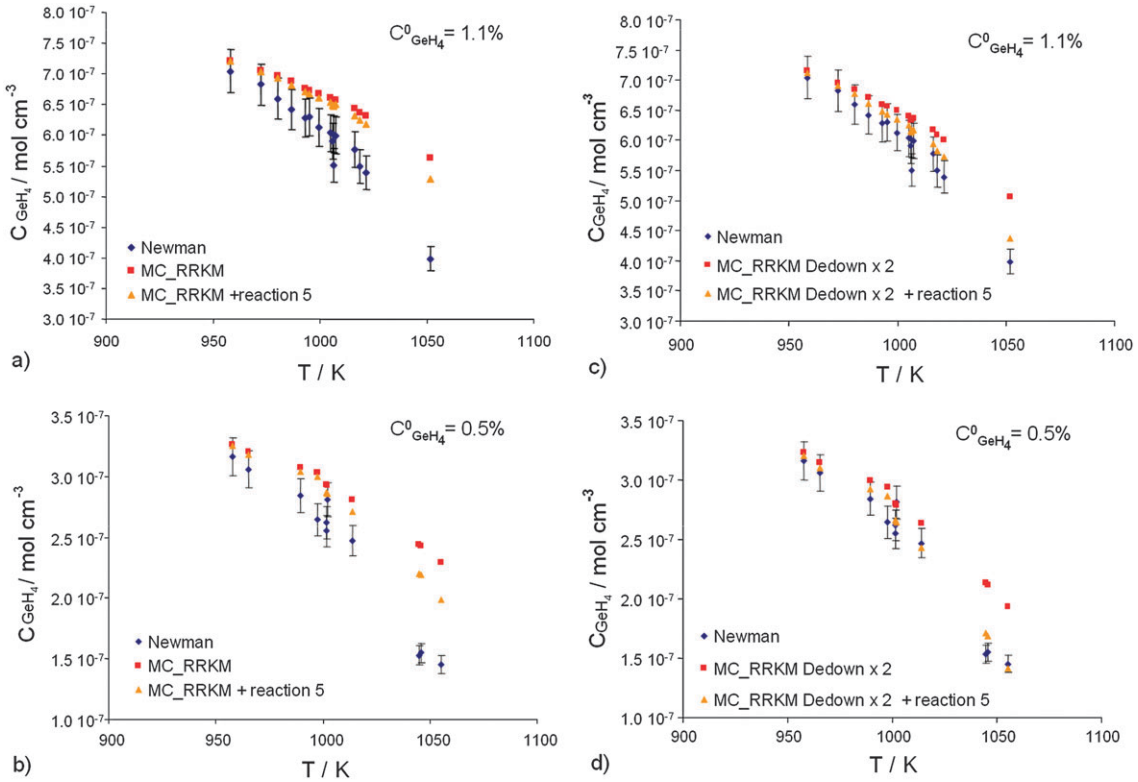

Fig. 7 Comparison of the calculated concentrations with experimental data measured after variable reaction times (240–390 μs) with an initial fraction of GeH_4 of 1.1% (a and c) and 0.5% (b and d) at a pressure of 1.5 bar. Points are experimental data, results reported as squares were obtained not considering reaction (5), while results sketched in triangles were obtained including reaction (5) in the kinetic scheme.

did not affect the computational results. This is determined by the relatively high concentration of GeH_4 used for the experiments (0.5–1% GeH_4 mixtures in Ar), in which decomposition leads to the formation of a concentration of Ge molecules sufficient to react quantitatively with the precursor.

The data reported in Fig. 4 show that the GeH_4 and GeH_2 decomposition rates are in their fall off regime for the whole temperature and pressure range considered in this study, which covers in practice all the operating conditions in which Ge films are deposited from this precursor. Since the accurate knowledge of these decomposition parameters is of practical importance in order to study the gas phase kinetics active during the deposition of Ge films, we have fitted the decomposition rate constant to the Troe form so that it is possible to calculate for any range of operating parameters the correct decomposition rates. The interpolated low pressure kinetic constant and FCent parameters are reported in Table 6.

Table 6 Fit of the GeH_4 and GeH_2 kinetic parameters to the Troe formalism: high pressure (s^{-1}), low pressure ($cm^3\ mol^{-1}\ s^{-1}$) and FC parameters for the broadening factor (T^{**} was set to 0 in the regression). Activation energies in kJ mol^{-1}

	A	n	E_a	T-range/K
GeH_4				
K_∞	6.4×10^{13}	0.272	221.90	300–2200
k_0	2.75×10^{48}	−9.055	263.35	1100–1700
	a	T^{***}	T^*	
Fcent	0.216	626.55	-2.59×10^7	1100–1700
GeH_2				
K_∞	6.02×10^{12}	0.203	163.5	300–2200
k_0	1.6×10^{26}	−3.06	175.6	1100–1700
	a	T^{***}	T^*	
Fcent	0.011	1.404×10^3	-5.427×10^2	1100–1700

Conclusions

The decomposition rate of GeH_4 and GeH_2 was studied through RRKM/ME simulations using structural and energetic parameters determined from *ab initio* simulations. Our calculations confirm that in the considered temperature and pressure ranges both reactions are in the fall off regime. It was found that GeH_2 decomposes faster than GeH_4 and that, at sufficiently high partial pressures, the Ge atoms so produced are likely to react with GeH_4 to enhance its decomposition.

A good agreement between experimental data and calculated GeH_4 and GeH_2 decomposition rates could be obtained assuming that the energy transfer parameter is $340 \times (T/298\ K)^{0.85}\ cm^{-1}$ for both GeH_4 and GeH_2. This parameter is in reasonable agreement with that used in several RRKM studies on the GeH_2 reactivity, in which it was adopted a temperature independent energy transfer parameter of 800 cm^{-1}.[53,54] Finally, despite the increase of the energy transfer parameter, our calculations still underpredict the GeH_2 decomposition rate by a factor of 1.6, well within the uncertainty range of these calculations, which have been estimated to be about a factor of 2 and 4 for the GeH_4 and GeH_2 decomposition reactions, respectively, due to the uncertainty of the calculated energies and transition state structures. Since in this case the validation of the computational results is based on the

comparison with a single set of experimental data and GeH_2 is an extremely reactive molecule, we think that further studies will be necessary to definitely assess the kinetic constant value of this reaction.

References

1 C. Cavallotti, M. Di Stanislao and S. Carra, *Prog. Cryst. Growth Charact. Mater.*, 2004, **48–49**, 123–165.
2 R. C. Binning and L. A. Curtiss, *J. Chem. Phys.*, 1990, **92**, 1860–1864.
3 S. D. Chambreau and J. S. Zhang, *Chem. Phys. Lett.*, 2002, **351**, 171–177.
4 D. Dakternieks, D. J. Henry and C. H. Schiesser, *Organometallics*, 1998, **17**, 1079–1084.
5 K. K. Das and K. Balasubramanian, *J. Chem. Phys.*, 1990, **93**, 5883–5889.
6 P. R. Duchowicz and C. J. Cobos, *J. Phys. Chem. A*, 2008, **112**, 6198–6204.
7 K. G. Dyall, *J. Chem. Phys.*, 1992, **96**, 1210–1217.
8 R. S. Grev, H. F. Schaefer III and K. M. Baeins, *J. Am. Chem. Soc.*, 1990, **112**, 9458–9467.
9 S. R. Gunn and L. G. Green, *J. Phys. Chem.*, 1961, **65**, 779–783.
10 J. Karolczak, W. W. Harper, R. S. Grev and D. J. Clouthier, *J. Chem. Phys.*, 1995, **103**, 2839–2849.
11 H. Koizumi, J. Z. Davalos and T. Baer, *Chem. Phys.*, 2006, **324**, 385–392.
12 Q. S. Li, R. H. Lu, Y. M. Xie and H. F. Schaefer III, *J. Comput. Chem.*, 2002, **23**, 1642–1655.
13 P. M. Mayer, J. F. Gal and L. Radom, *Int. J. Mass Spectrom.*, 1997, **167**, 689–696.
14 P. N. Noble and R. Walsh, *Int. J. Chem. Kinet.*, 1983, **15**, 547–560.
15 A. Ricca and C. W. Bauschlicher, *J. Phys. Chem. A*, 1999, **103**, 11121–11125.
16 B. Ruscic, M. Schwarz and J. Berkowitz, *J. Chem. Phys.*, 1990, **92**, 1865–1875.
17 M. D. Su and S. Y. Chu, *J. Am. Chem. Soc.*, 1999, **121**, 11478–11485.
18 M. D. Su and S. Y. Chu, *J. Am. Chem. Soc.*, 1999, **121**, 4229–4237.
19 M. D. Su and S. Y. Chu, *J. Chin. Chem. Soc. (Taipei)*, 2000, **47**, 135–139.
20 L. M. Wang and J. S. Zhang, *J. Phys. Chem. A*, 2004, **108**, 10346–10353.
21 S. Yockel, B. Mintz and A. K. Wilson, *J. Chem. Phys.*, 2004, **121**, 60–77.
22 Y. Wu, Y. H. Ding, J. F. Xiao, Z. S. Li, X. R. Huang and C. C. Sun, *J. Comput. Chem.*, 2002, **23**, 1366–1374.
23 K. J. Reed and J. I. Brauman, *J. Chem. Phys.*, 1974, **61**, 4830–4838.
24 J. Berkowitz, G. B. Ellison and D. Gutman, *J. Phys. Chem.*, 1994, **98**, 2744–2765.
25 H. Simka, M. Hierlemann, M. Utz and K. F. Jensen, *J. Electrochem. Soc.*, 1996, **143**, 2646–2654.
26 C. G. Newman, J. Dzarnoski, M. A. Ring and H. E. O'Neal, *Int. J. Chem. Kinet.*, 1980, **2**, 661–670.
27 V. N. Smirnov, *Kinet. Katal.*, 2007, **48**, 615–619.
28 V. N. Votintsev, I. S. Zaslonko, V. S. Mikheev and V. N. Smirnov, *Kinet. Katal.*, 1986, **26**, 1114–1119.
29 A. Barbato, C. Seghi and C. Cavallotti, *J. Chem. Phys.*, 2009, **130**, 074108.
30 V. N. Votintsev, I. S. Zaslonko, V. S. Mikheev and V. N. Smirnov, *Kinet. Katal.*, 1985, **26**, 1297–1302.
31 R. G. Gilbert and S. C. Smith, *Theory of Unimolecular and Recombination Reactions*, Blackwell Scientific Publications, Oxford, 1990.
32 A. D. Becke, *J. Chem. Phys.*, 1993, **98**, 5648–5652.
33 C. Lee, W. Yang and R. G. Parr, *Phys. Rev. B: Condens. Matter*, 1988, **37**, 785.
34 A. K. Wilson, D. E. Woon, K. A. Peterson and T. H. Dunning, *J. Chem. Phys.*, 1999, **110**, 7667–7676.
35 K. Raghavachari, G. W. Trucks, J. A. Pople and M. Head-Gordon, *Chem. Phys. Lett.*, 1989, **157**, 479.
36 J. M. L. Martin, *Chem. Phys. Lett.*, 1996, **259**, 669–678.
37 J. Finley, P. A. Malmqvist, B. O. Roos and L. Serrano-Andres, *Chem. Phys. Lett.*, 1998, **288**, 299–306.
38 B. O. Roos, K. Andersson, M. P. Fulscher, P. A. Malmqvist, L. SerranoAndres, K. Pierloot and M. Merchan, *Adv. Chem. Phys.*, 1996, **93**, 219–331.
39 M. J. Frisch, G. W. Trucks, H. B. Schlegel, G. E. Scuseria, M. A. Robb, J. R. Chesseman, J. A. Montgomery, Jr., T. Vreven, K. N. Kudin, J. C. Burant, J. M. Millam, S. S. Iyengar, J. Tomasi, V. Barone, B. Mennucci, M. Cossi, G. Scalmani, N. Rega, G. A. Petersson, H. Nakatsuji, M. Hada, M. Ehara, K. Toyota, R. Fukuda, J. Hasegawa, M. Ishida, T. Nakajima, Y. Honda, O. Kitao, H. Nakai, M. Klene, X. Li, J. E. Knox, H. P. Hratchian, J. B. Cross, V. Bakken, C. Adamo, J. Jaramillo, R. Gomperts, R. E. Stratmann, O. Yazyev, A. J. Austin, R. Cammi, C. Pomelli, J. W. Ochterski, P. Y. Ayala, K. Morokuma, G. A. Voth, P. Salvador, J. J. Dannenberg, V. G. Zakrzewski, S. Dapprich, A. D. Daniels, M. C. Strain, O. Farkas, D. K. Malick, A. D. Rabuck, K. Raghavachari, J. B. Foresman, J. V. Ortiz, Q. Cui, A. G. Baboul, S. Clifford, J. Cioslowski, B. B. Stefanov, G. Liu, A. Liashenko, P. Piskorz, I. Komaromi, R. L. Martin, D. J. Fox, T. Keith, M. A. Al-Laham, C. Y. Peng, A. Nanayakkara, M. Challacombe, P. M. W. Gill, B. Johnson, W. Chen, M. W. Wong, C. Gonzalez and J. A. Pople, *Gaussian 03 (Revision B.05)*, Gaussian, Inc., Pittsburgh, PA, 2003.
40 *MOLPRO version 2008.1*, H.-J. Werner, P. J. Knowles, R. Lindh, F. R. Manby, M. Schütz, P. Celani, T. Korona, A. Mitrushenkov, G. Rauhut, T. B. Adler, R. D. Amos, A. Bernhardsson, A. Berning, D. L. Cooper, M. J. O. Deegan, A. J. Dobbyn, F. Eckert, E. Goll, C. Hampel, G. Hetzer, T. Hrenar, G. Knizia, C. Köppl, Y. Liu, A. W. Lloyd, R. A. Mata, A. J. May, S. J. McNicholas, W. Meyer, M. E. Mura, A. Nicklaß, P. Palmieri, K. Pflüger, R. Pitzer, M. Reiher, U. Schumann, H. Stoll, A. J. Stone, R. Tarroni, T. Thorsteinsson, M. Wang and A. Wolfsee http://www.molpro.net.
41 J. A. Miller, S. J. Klippenstein and C. Raffy, *J. Phys. Chem. A*, 2002, **106**, 4904–4913.
42 J. N. Harvey, *Phys. Chem. Chem. Phys.*, 2007, **9**, 331–343.
43 N. Matsunaga, S. Koseki and M. S. Gordon, *J. Chem. Phys.*, 1996, **104**, 7988–7996.
44 C. Zener, *Proc. R. Soc. London, Ser. A*, 1932, **137**, 696–702.
45 A. Berning, M. Schweizer, H. J. Werner, P. J. Knowles and P. Palmieri, *Mol. Phys.*, 2000, **98**, 1823–1833.
46 S. E. Boganov, M. P. Egorov, V. I. Faustov, L. V. Krylova, O. M. Nefedov, R. Becerra and R. Walsh, *Russ. Chem. Bull.*, 2005, **54**, 483–511.
47 R. Becerra, S. E. Boganov, M. P. Egorov, V. I. Faustov, O. M. Nefedov and R. Walsh, *Can. J. Chem.*, 2000, **78**, 1428–1433.
48 V. P. Glushko, L. V. Gurvich, G. A. Bergman, I. V. Veits, V. A. Medvedv, G. A. Khachkuruzov and V. S. Yungman, *Termodinamicheski Svoistva Individual' nikh Veshchestv*, Nauka, Moskow, 1979.
49 R. Becerra, S. Boganov and R. Walsh, *J. Chem. Soc., Faraday Trans.*, 1998, **94**, 3569–3572.
50 K. Matsumoto, S. J. Klippenstein, K. Tonokura and M. Koshi, *J. Phys. Chem. A*, 2005, **109**, 4911–4920.
51 A. Dollet and S. de Persis, *J. Anal. Appl. Pyrolysis*, 2007, **80**, 460–470.
52 T. Tanaka, M. Hiramatsu, M. Nawata, A. Kono and T. Goto, *J. Phys. D: Appl. Phys.*, 1994, **27**, 1660–1663.
53 R. Becerra, S. E. Boganov, M. P. Egorov, V. I. Faustov, V. M. Promyslov, O. M. Nefedov and R. Walsh, *Phys. Chem. Chem. Phys.*, 2002, **4**, 5079–5087.
54 R. Becerra, S. E. Boganov, M. P. Egorov, V. I. Faustov, I. V. Krylova, O. M. Nefedov, V. M. Promyslov and R. Walsh, *Phys. Chem. Chem. Phys.*, 2007, **9**, 4395–4406.

